Static stability and load capacity of pyramidal trusses

Murillo V. B. Santana[1,⋆], *Paulo B.* Gonçalves[1], and *Ricardo A. M.* Silveira[2]

[1] *Departamento de Engenharia Civil - Pontifícia Universidade Católica do Rio de Janeiro*
[2] *Departamento de Engenharia Civil - Escola de Minas - Universidade Federal de Ouro Preto*

Abstract. The analysis of pyramidal trusses has an immediate practical interest since these structures are currently used in many present-day civil constructions, either as main parts or a constitutive element. They can be used to represent tripod-like structures, cap of masts, tower cranes, big span roofs, and even a portion of a single-layer geodesic dome or of a generic-shaped reticulated shell. This paper examines the nonlinear static stability and load capacity for a simple class of space trusses in the shape of a regular pyramid. Joints located at the vertices of the base polygon are fixed while the joint at the apex is subjected to static loads acting in either the vertical direction, in the horizontal plane, or along a generic oblique direction. Despite their apparent simplicity, these structural systems exhibit a wide variety of post-critical responses, not exhausted by the classical snapping and bifurcation phenomena. In addition to regular primary and secondary branches, the equilibrium paths may include neutral branches, namely branches entirely composed of bifurcation or limit points. The analysis is conducted using the Finite Element Method together with a corotational formulation for the bars. The numerical results are validated in the elastic domain using the closed-form solutions found in literature.

1 Introduction

In this work the large displacement response of a class of space trusses in the shape of a regular pyramid is studied using a finite element formulation. Pyramidal trusses possess an immediate practical interest since they are currently used in many present-day civil constructions, either as main parts or as minor elements. For instance, if the number n of the composing bars is 3, we find a common tripod-like structure loaded on its upper joint. For n = 4 and a large height to base ratio, the truss may represent the cap of a mast or, if the load acts transversally, the extremity of a three-dimensional cantilever beam or of the jib of a tower crane. Finally, for n = 5 or n = 6 and a small height to base ratio, the truss may represent a molecule of a single-layer geodesic dome or of a generic-shaped reticulated shell [6].

The paper is organized as follows: in Section 2, the system equilibrium equations are posed considering an elastic response and thick elements. Section 3 presents the nonlinear effects in the structural response: snap-through and bifurcation. Finally, some concluding remarks are given in Section 4.

2 Analytic Model

The pyramidal truss considered in this study is shown in Fig. 1. It consist of $n \geq 3$ bars pinned at the joints and equally spaced so that the base nodes form a regular polygon of n sides simply supported and equally separated at the regular base Γ and connected at the apex node. The pyramid has height H, base radius B and bar's length $L = \sqrt{B^2 + H^2}$.

In the initial configuration, the apex and i^{th} base nodes are located at $\begin{bmatrix} 0 & 0 & H \end{bmatrix}^T$ and $\begin{bmatrix} B\cos(\theta_i) & B\sin(\theta_i) & 0 \end{bmatrix}^T$, respectively, with $\theta_i = 2\pi i/n$. The apex node is free to move and it's position is given by $\mathbf{x} = \begin{bmatrix} x & y & z \end{bmatrix}^T$ or, in a cylindrical coordinates system, by $\mathbf{x} = \begin{bmatrix} \theta & r & z \end{bmatrix}^T$. The structure is subjected to a load $\mathbf{p} = \lambda \begin{bmatrix} 0 & 0 & p_z \end{bmatrix}^T$. Here, it is assumed that all joints behave as ideal frictionless hinges, so that no moments are generated in them by nodal loads.

Following [6], considering no imperfections, the current length of the bar connecting the apex and i^{th} nodes is:

$$l_i^2 = r^2 - 2rB\cos(\theta - \theta_i) + B^2 + z^2 \tag{1}$$

As in the bar element, the Green-Lagrange strain is given by $\varepsilon_i = (l_i^2 - L^2)/(2L^2)$ and thus, considering an elastic material response, the axial force is $N_i = (l_i/L)\, EA\varepsilon_i$. The system internal $W(\mathbf{x})$ and external $V(\mathbf{x}, \lambda)$ potential energies can be written as:

$$W(\mathbf{x}) = \frac{nEA}{8L^3}\left[\left(r^2 + z^2 - H^2\right)^2 + 2B^2 r^2\right] \tag{2}$$

$$V(\mathbf{x}, \lambda) = \lambda p_z (z - H) \tag{3}$$

⋆ e-mail: murilvbs@aluno.puc-rio.br

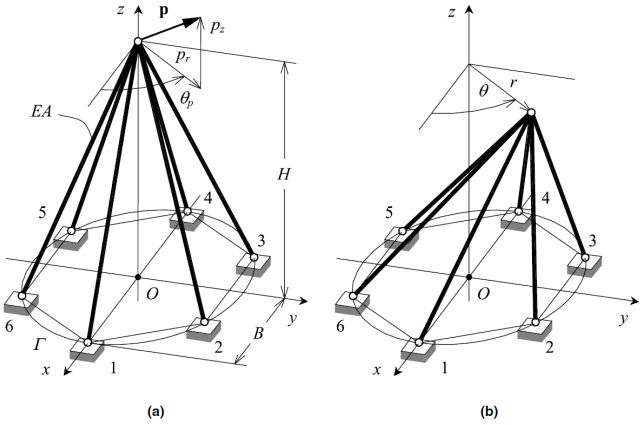

Figure 1. Pyramidal truss: (a) Initial and (b) Current equilibrium configuration. Source [6]

The system's total potential energy is given by $\Pi(\mathbf{x}, \lambda) = W(\mathbf{x}) - V(\mathbf{x}, \lambda)$. Applying the minimum potential energy principle, the nonlinear equilibrium equations are obtained as:

$$\mathbf{r}(\mathbf{x}, \lambda) = \frac{\partial \Pi}{\partial \mathbf{x}} = \mathbf{F}_i(\mathbf{x}) - \mathbf{F}_e(\lambda) = \mathbf{0} \tag{4}$$

where the system internal $\mathbf{F}_i(\mathbf{x})$ and external $\mathbf{F}_e(\lambda)$ force vectors are given by:

$$\mathbf{F}_i(\mathbf{x}) = \frac{nEA}{2L^3}\begin{bmatrix} x\mu_1^2 & y\mu_1^2 & z\mu_2^2 \end{bmatrix}^T \tag{5}$$

$$\mathbf{F}_e(\lambda) = \lambda\begin{bmatrix} 0 & 0 & p_z \end{bmatrix}^T \tag{6}$$

In the above equations we have $\mu_1^2 = r^2 + z^2 + B^2 - H^2$ and $\mu_2^2 = r^2 + z^2 - H^2$. The system stiffness matrix is obtained by taking the variation of the internal force vector in Eq. 5:

$$\mathbf{K}(\mathbf{x}) = \frac{\partial \mathbf{F}_i}{\partial \mathbf{x}} = \frac{nEA}{2L^3}\begin{bmatrix} 2x^2 + \mu_1^2 & 2xy & 2xz \\ 2xy & 2y^2 + \mu_1^2 & 2yz \\ 2xz & 2yz & 2z^2 + \mu_2^2 \end{bmatrix} \tag{7}$$

3 Analysis

In this section, the static stability and load capacity of the system are studied. The effects of two types of nonlinear behavior are considered: snap-through and bifurcation. The snap-through behavior is characterized by two limit points along the nonlinear equilibrium path, where a dynamic jump to an inverted position occurs. This buckling behavior is typical of very shallow systems, where jump can occur in the elastic range.

For deeper structures, however, it's possible that the primary equilibrium path becomes unstable before the structure reaches the limit points. In such cases, the truss looses stability through an unstable symmetric bifurcation, where the secondary path connects this critical point to its mirror inverted position. This bifurcation is associated to an asymmetric buckling mode. Again after reaching the bifurcation point the structure jumps to an inverted configuration.

Along both paths and during the dynamic jump the bars are subjected to compressive axial forces, which can become greater than the Euler's buckling load [2] or the stresses may reach the material elastic limits [5], leading to an inelastic nonlinear response. In such cases, the local instability of the bars and the plastic behavior of the material may influence the load carrying capacity of the structure. In addition, when subjected to unexpected loads, it's possible that the structure suffers members loss. The number and the way that the that the system losses it's elements may have great influence in it's stability and load capacity.

In all the numerical models, the pyramidal truss has $n = 6$ bars and base radius $B = 7.00$m. The structure height H is chosen depending on the nonlinear effect studied. Also, the bars have a hollow circle cross section with diameter $d = 508.0$mm and thickness $t = 12.7$mm. The material has an elastic modulus $E = 200$GPa and yield stress $\sigma_y = 400$MPa. The reference load is taken as $p_z = -(H/L)^3\,(nEA/2)$. The solution of the nonlinear equations is obtained through an incremental - iterative Newton - Raphson process [3] associated with an arc-length method [4]. In addition, the following non-dimensional parameters are used in the analysis $\bar{z} = z/H$, $\bar{r} = r/H$, $\alpha = B/H$, $\beta = L/H = \sqrt{1+\alpha^2}$ and $\overline{\omega}_i = \omega_i/\omega_{1,0}$.

The static global behavior of the pyramidal lattice truss is mainly governed by the topology of the total potential energy. In terms of non-dimensional quantities, substituting the parameters defined before in Eq. (2), the static potential energy of the structure ($\overline{\Pi}$) is given by:

$$\overline{\Pi} = \Pi/(p_z H) \tag{8}$$

$$\overline{\Pi} = \left[\left(\bar{r}^2 + \bar{z}^2 - 1\right)^2 + 2\alpha^2\bar{r}^2\right]/4 - \lambda\,(\bar{z} - 1) \tag{9}$$

The static unloaded equipotential curves for the three selected values of α are shown in Fig. 2. For $\alpha = 0.80 < 1.00$, Fig. 2(a), the potential energy displays five equilibrium positions, the origin, a local maximum (unstable), two additional equilibrium positions along the $\bar{z}$ axis at $\bar{z} = \pm 1.00$, corresponding to two local minima (stable), and two additional equilibrium positions along the $\bar{r}$ axis at $\bar{r} = \pm\sqrt{1-\alpha^2}$, corresponding to two symmetric saddles (unstable).

At $\alpha = 1.00$, Fig. 2(b), the two saddles coalesce with the maximum, leading to a degenerated saddle, with the only eigenvector in the direction of the axis, reducing the number of equilibrium positions to three. For $\alpha = 1.20 > 1.00$, Fig. 2(c), there are only three equilibrium positions, a saddle (unstable) at the origin and two symmetric minimum (stable) along the $\bar{z}$ axis. So, $\alpha = 1.00$ corresponds to a critical value separating two types of global behavior.

The static loaded equipotential curves with $\alpha = 0.80$ and $\lambda = 0.25$ are shown in Fig. 3. The presence of a load changes the topology of the total potential energy, modifying the number of solutions, the position of the equilibrium points on the $(\bar{r}, \bar{z})$ plane and their stability. The load breaks the symmetry of potential with respect to the $\bar{r}$ axis, shifting the equilibrium points away from it.

One should have in mind that Figs. 2 and 3 represents the cross sections of the four dimensional phase-space of

the conservative system and that the stable and unstable manifolds of the saddles separate the initial conditions that lead to bounded solutions surrounding the stable equilibrium positions of the unloaded structure. The knowledge of these frontiers helps the designer to separate the phase space into safe and unsafe domains and evaluate the degree of safety of the system. In the following, a parametric analysis of the truss under vertical and horizontal loads is presented.

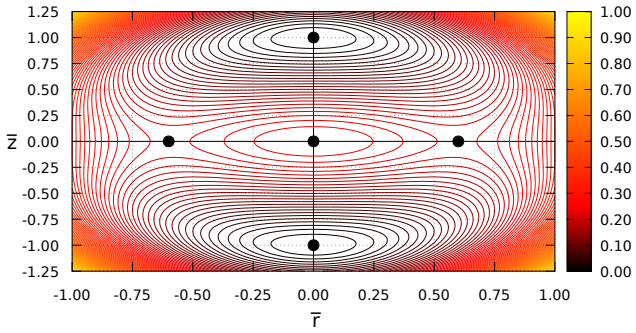

(a) $\alpha = 0.80$

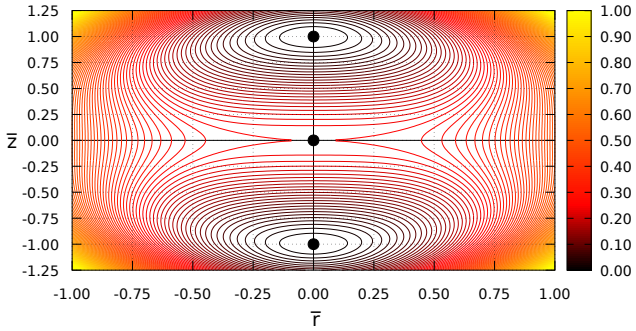

(b) $\alpha = 1.00$

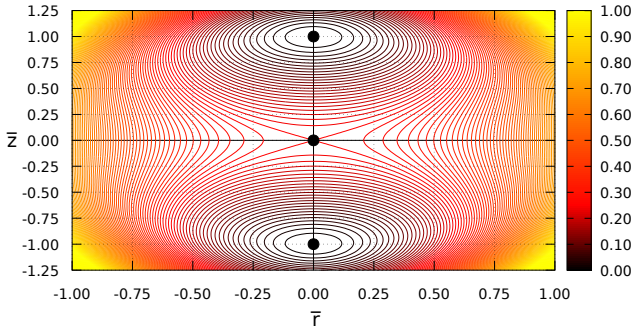

(c) $\alpha = 1.20$

Figure 2. Unloaded equipotential energy curves.

3.1 Snap-through

Initially the elastic symmetric response of the system (nonlinear primary path) subjected to a vertical load at the apex node is considered, for which case we have $r = 0$ and,

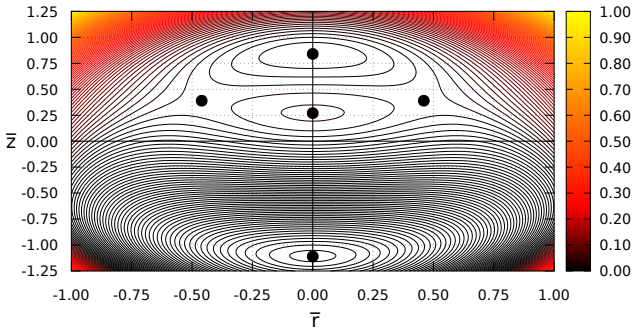

Figure 3. Loaded equipotential energy curves.

from Eqs. 4-6:

$$\lambda = \bar{z}\left(1 - \bar{z}^2\right) \tag{10}$$

The differentiation of the previous equation give the limit points $(\bar{z}_l^v, \lambda_l^v)$ as:

$$\bar{z}_l^v = \pm\sqrt{3}/3 \quad \lambda_l^v = \pm 2\sqrt{3}/9 \tag{11}$$

From the stiffness (Eq. 7), the instability conditions are $|\bar{z}| > \sqrt{3}/3$ and $|\bar{z}| > \sqrt{1-\alpha^2}$. The first condition is associated with the limit points of the snap-through behavior while the second one only appears in deep systems and is associated with the bifurcation behavior (Sec. 3.2), for shallow systems this condition is automatically satisfied. The equilibrium path and limit points with $\alpha = 1.20$ are shown in Fig. 4.

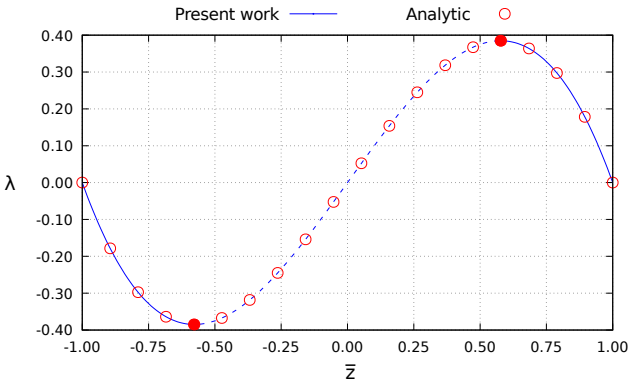

Figure 4. Equilibrium path: snap - through ($\alpha = 1.20$).

3.2 Bifurcation

Now we study the bifurcation (nonlinear secondary path) response of the system. For the elastic structure we consider a $0.1\%H$ imperfection in the x direction of the apex node for the numerical analysis. Considering $r \neq 0$ and combining the x and y components in Eqs. **??**-6 we have $r = \sqrt{H^2 - B^2 - z^2}$ and:

$$\lambda = \alpha^2\bar{z} \tag{12}$$

The bifurcation points $(\bar{z}_b^v, \lambda_b^v)$ are the intersections of the equilibrium paths in Eqs. 10 and 12:

$$\bar{z}_b^v = \pm\sqrt{1-\alpha^2} \quad \lambda_b^v = \pm\alpha^2\sqrt{1-\alpha^2} \tag{13}$$

The previous equations provides the bifurcation condition as $H \geq H_b = B$. In addition, from Eqs. (11) and (13), the limit point $(\bar{z}_l^v, \lambda_l^v)$ and bifurcation point $(\bar{z}_b^v, \lambda_b^v)$ under vertical load coincide if $\alpha = \sqrt{6}/3$. For $\alpha > \sqrt{6}/3$, the bifurcation point appears on the unstable part of the nonlinear equilibrium path, without influence on the load capacity but changing the static behavior. The bifurcation point disappears for $\alpha > 1$.

The apex node movement is illustrated in Fig. 5. The equilibrium path is shown in Fig. 6 for $\alpha = 0.7$. We can notice that, in the secondary branch, the system loses stability, but later recovers it, returning to the primary branch, as the compressive axial force in the bars is reduced.

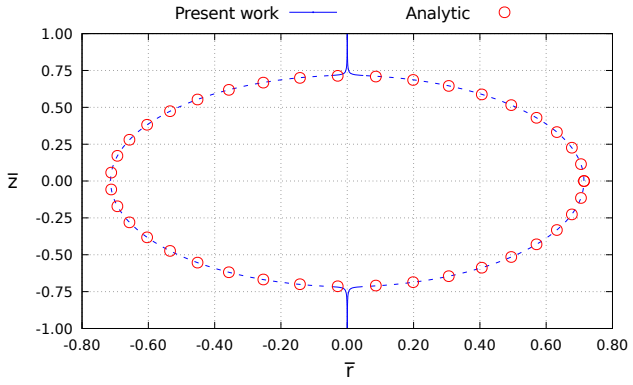

Figure 5. Apex movement: bifurcation ($\alpha = 0.7$).

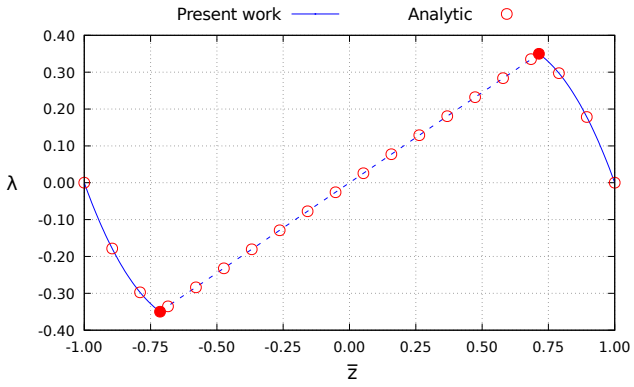

Figure 6. Equilibrium path: bifurcation ($\alpha = 0.7$).

4 Conclusions

In this work, the stability and load capacity for space trusses in the shape of a regular pyramid was studied. Using a Finite Element formulation, the numeric response was first validated with the analytical one proposed by [6] in the elastic range for the system snap-through and bifurcation. The snap-through effect is present regardless of the system parameters, creating limit load points and instability. For deep structures, global instability may appear as a bifurcation in the equilibrium path.

References

[1] Battini, J. M., Pacoste, C., Comput. Methods Appl. Mech. Engrg, 191, 1755–1789 (2002)
[2] Bazzucchi, F., Manuello, A., Carpinteri, A., International Journal of Non–Linear Mechanics, 88, 11-20 (2017)
[3] Crisfield, M. A., Wiley, Chichester (1991)
[4] Krenk, S., Cambridge University Press, New York (2009)
[5] Jiang, X. M., Chen, H., Liew, J. Y. R., Journal of Constructional Steel Research, 58, 193–212 (2002)
[6] Ligarò, S. S., Valvo, P. S., International Journal of Solids and Structures, 43, 4867–4887 (2006)